(MMC) photosynthesis. Measurements of MMC net productivity (NP) and DIC budgets under different conditions enabled determination of the depletion factor (Φ), which is defined as

$$\Phi[\mathrm{d}^{-1}] = \frac{\mathrm{NP}[\mathrm{mol{\cdot}m^{-2}{\cdot}d^{-1}}]}{\mathrm{DIC}[\mathrm{mol{\cdot}m^{-3}}]Z[\mathrm{m}]},$$

and has units of per day. The observations showed that the onset of $\delta^{13}C$ depletion was when $\Phi \sim 0.2$ per day. Substituting this value of Φ into the equation together with the normal values for MMC net production (250 mg of C per square meter per day) and DIC concentration (1 to 4 mmol/l) yield an estimate for maximum lake depth (Z) during low stand of 10 to 40 cm.

19. G. L. Possehl, in *South Asian Archeology 1991*, A. Gail and G. Mevisson, Eds. (Steiner Verlag, Stuttgart, 1993), pp. 231–250.
20. Vishnu-Mittre, *Geophytology* **4** (no. 1), (1974); *Paleobotanist* **25**, 549 (1978); V. N. Misra, in *Frontiers of the Indus Civilization*, B. B. Lal and S. P. Gupta, Eds. (Books and Books, New Delhi, 1984), pp. 461–489; B. K. Thapar, *Recent Archeological Discoveries in India* (The Centre for East Asian Cultural Studies, United Nations Educational, Scientific and Cultural Organization, 1995); M.-A. Courty, in *Ancient People and Landscape*, E. Johnson, Ed. (Texas Univ. Press, Lubbock, 1995), pp.105–126.
21. S. J. Burns, A. Matter, N. Frank, A. Mangini, *Geology* **26**, 499 (1998).
22. M. Stuiver and P. J. Reimer, *Radiocarbon* **35**, 215 (1993).

23. Supported by National Science Foundation (NSF) grants EAR-9104489 and EAR-9417896 to V.R.B. and EAR-9418989 to L.L.E. Additional support to L.L.E. was provided by NSF Post-Doctoral Fellowship grant EAR-9202498, conducted at the Earth System Science Center, Pennsylvania State University. ^{14}C analyses were conducted at and partially funded by the NSF, University of Arizona AMS laboratory. We thank A. K. Singhvi for fruitful discussions. M. Shmida helped with drafting and I. Zicha with laboratory analyses.

4 September 1998; accepted 26 February 1999

Clinoenstatite in Alpe Arami Peridotite: Additional Evidence of Very High Pressure

K. N. Bozhilov, H. W. Green II, L. Dobrzhinetskaya

Observations by transmission electron microscopy show that lamellae of clinoenstatite are present in diopside grains of the Alpe Arami garnet lherzolite of the Swiss Alps. The simplest interpretation of the orientation, crystallography, and microstructures of the lamellae and the phase relationships in this system is that the lamellae originally exsolved as the high-pressure C-centered form of clinoenstatite. These results imply that the rocks were exhumed from a minimum depth of 250 kilometers before or during continental collision.

In fresh samples of the Alpe Arami garnet lherzolite of the Swiss Alps, the oldest generation of olivine contains up to 1% by volume rod-shaped precipitates of $FeTiO_3$ parallel to [010] of olivine and up to ~0.2% by volume tabular chromite precipitates parallel to (100) (*1*). These oxide precipitates are much more abundant than reported previously (*2*) and suggest much greater solubility of highly charged cations than has been measured in mantle olivine (*3*). These precipitates are older than the dislocation microstructure (*4*) and therefore predate the Alpine deformation. This older generation of olivine exhibits a unique lattice-preferred orientation (LPO) (*5*) that is incompatible with the deformation mechanisms known to operate in olivine in other naturally deformed peridotites (*6*) and in the laboratory (*7*). Partial recrystallization during Alpine deformation of this peridotite has produced a younger generation of olivine that contains no oxide inclusions, a normal LPO associated with a new foliation, and a normal dislocation substructure (*5*). These observations led Dobrzhinetskaya *et al.* (*1*) to infer an extreme depth of origin (>300 km) of the peridotite, a proposition that has been controversial because the high TiO_2 contents of the olivine inferred from volume fraction measurements of the precipitates could not be confirmed by broad-beam electron microprobe measurements (*8*). Here we confirm an earlier report of clinoenstatite lamellae exsolved from diopside in these rocks (*9*). Detailed analysis of these lamellae indicates that the phase originally precipitated was probably the high-pressure monoclinic polymorph of enstatite, which is stable only at depths exceeding 250 km at upper mantle temperatures.

Twenty diopside crystals from specimens that also contain olivine exhibiting extensive precipitation of oxides were chosen for examination by analytical transmission electron microscopy (TEM) (*10*). The diopsides were selected from two microenvironments: within and adjacent to garnets and scattered in the olivine + enstatite matrix. The latter group of diopsides shows a nearly perfect substructure other than widely spaced retrograde lamellae of amphibole (*11*). The former exhibit abundant clinoenstatite lamellae and ubiquitous thin (010) amphibole slabs (Fig. 1, A and B) (*12*). Locally, these diopsides also contain numerous chromite exsolution lamellae and rare orthoenstatite lamellae (*11*). The density of clinoenstatite lamellae varies from about 1 to 5% by volume (Fig. 1A).

The clinoenstatite lamellae [space group (SG) $P2_1/c$] and diopside host (SG $C2/c$) share the *b* axis, with their *c* axes subparallel at an angle of about 2° (Fig. 1D). The lamellae are oriented approximately parallel to (401) of diopside, making an angle of 20° to 24° with the (100) planes of both phases (Figs. 1C). Brightfield images exhibit blotchy contrast within the lamellae on a wavelength of a few nanometers, which is not observed in the diopside host (Fig. 1C). Darkfield imaging of the lamellae with $h + k =$ even reflections shows the same mottling; alternating darker and lighter contrast regions are elongated across the lamellae (Fig. 2A). In contrast, imaging with $h + k =$ odd shows generally equidimensional domains that are smaller and exhibit much higher contrast (Fig. 2B). High-resolution TEM (HRTEM) imaging down the *b* axis (Fig. 3) clearly shows that the contrast is mottled within the lamella and that the spacing between (100) planes of the primitive lattice of the clinoenstatite lamella is 9 Å (SG $P2_1/c$) as compared to the ~4.5 Å lattice fringes in diopside (SG $C2/c$). Examination of Fig. 3 also shows that the dark/light mottled contrast that was visible in both brightfield and $h + k =$ even imaging is a result primarily of elastic distortion of the lattice. Closer examination, however, shows numerous places where the (100) lattice fringes are systematically offset by *a*/2. Many of these sites of lattice offset are at the margins of the regions of alternating contrast, but others do not show such correlation (*13*). The arrays of lattice terminations generally border domains with apparent ~4.5 Å spacing rather than forming sharply defined interfaces. These could be either true relict domains of $C2/c$ pyroxene or, more likely because of their small size, regions where the surfaces of lattice offset are inclined with respect to the beam direction [010], causing partial overlap of neighboring domains. These observations, coupled with the marked differences in darkfield imaging with $h + k =$ odd or even, are consistent with the interpretation that regions of lattice fringe offset constitute antiphase boundaries, and the regions between them are antiphase domains related by displacement vector $1/2(a + b)$. Examination of the interfaces between lamellae and host on all scales shows that they lack misfit dislocations; they exhibit crystallographically controlled steps accompanied by small adjustments of the lattice fringes as they cross the boundary (Fig. 3). Thus, the boundaries are coherent.

The compositions of the studied crystals as determined by analytical electron microscopy are as follows: host diopside, $(Ca_{0.94}Na_{0.06}Mg_{0.84}Fe_{0.08}Cr_{0.03}Al_{0.04}Ti_{0.01})$-

---

Institute of Geophysics and Planetary Physics and Department of Earth Sciences, University of California, Riverside, CA 92521, USA.

$Si_{2.00}O_6$; clinoenstatite lamellae, $(Mg_{1.57}Fe_{0.25}Na_{0.03}Al_{0.02}Ca_{0.14})Si_{2.00}O_6$. Diopside crystallizes in SG *C*2/*c*, whereas pyroxenes with low calcium contents are known to crystallize in five different polymorphs: protoenstatite (SG *Pbcn*), orthoenstatite (Oren; SG *Pbca*), low clinoenstatite (Lclen; SG $P2_1/c$), high-temperature clinoenstatite (HTclen; SG *C*2/*c*), and high-pressure clinoenstatite (HPclen; SG *C*2/*c*) (*14*). Although HTclen and HPclen have the same SG, they differ in density and in structure (*14*). In experiments with Fe-poor systems, neither HTclen nor HPclen has been quenched to room temperature and pressure; both undergo spontaneous and rapid displacive transformations to Lclen (*14*). This result means that the presence of Lclen in our specimens does not necessarily signify that it precipitated directly from diopside; additional information is necessary to determine which of the low-calcium pyroxenes was the originally precipitating phase.

There are four possibilities for the origin of the Lclen lamellae in diopside: (i) direct exsolution of Lclen, (ii) exsolution of Oren with later transformation to Lclen by shearing or reconstructive growth, (iii) exsolution of HTclen with later transformation to Lclen, or (iv) exsolution of HPclen with later transformation to Lclen.

Direct exsolution of Lclen is highly unlikely because of the evidence for antiphase domains within the lamellae. These domains indicate that a precursor phase transformed to the Lclen structure by a displacive transformation; the crystallographic displacement implied by the offsets of lattice fringes across the domain boundaries is consistent with a precursor having SG *C*2/*c* (*15–17*). In addition, at the low temperatures where direct precipitation of Lclen might occur, diffusive cation exchange between phases would be inhibited, and the observed composition of diopside host and lamellae would be a reliable indicator of the composition at the time of exsolution. The recalculated diopside host composition (1 to 3% "enstatite") is such that exsolution would not occur (*18*).

Transformation of Oren to Lclen is a well-documented process (*14*, *15*, *19*). However, the microstructures that we observed contradict this mechanism. Oren always exsolves from diopside on (100) planes (including the rare Oren lamellae found in this study in the same crystals as contain the clinoenstatite lamellae). The Oren→Lclen transformation is reconstructive, involving breaking of strong bonds and rearranging of the structure. The relationship between the SGs of these two polymorphs precludes the formation of antiphase domains. Mechanical transformation of Oren to Lclen by a mechanism closely similar to mechanical twinning (*20*) is accomplished by partial dislocations traveling on (100) planes. Therefore, if the lamellae originally formed parallel to (100), shear transformation conceivably could have formed Lclen, but it could not have rotated the lamellae out of the (100) orientation and could not have led to the development of antiphase domains. In addition, such a mechanism is typically characterized by the extensive presence of stacking faults and twins in the resulting Lclen. The Lclen lamellae in our samples are free of such defects. At minimum, the partial dislocations that effected the transformation would have to be preserved at the boundaries of the lamellae—dislocations for which there is no evidence.

HTclen has SG *C*2/*c*, hence, based solely on

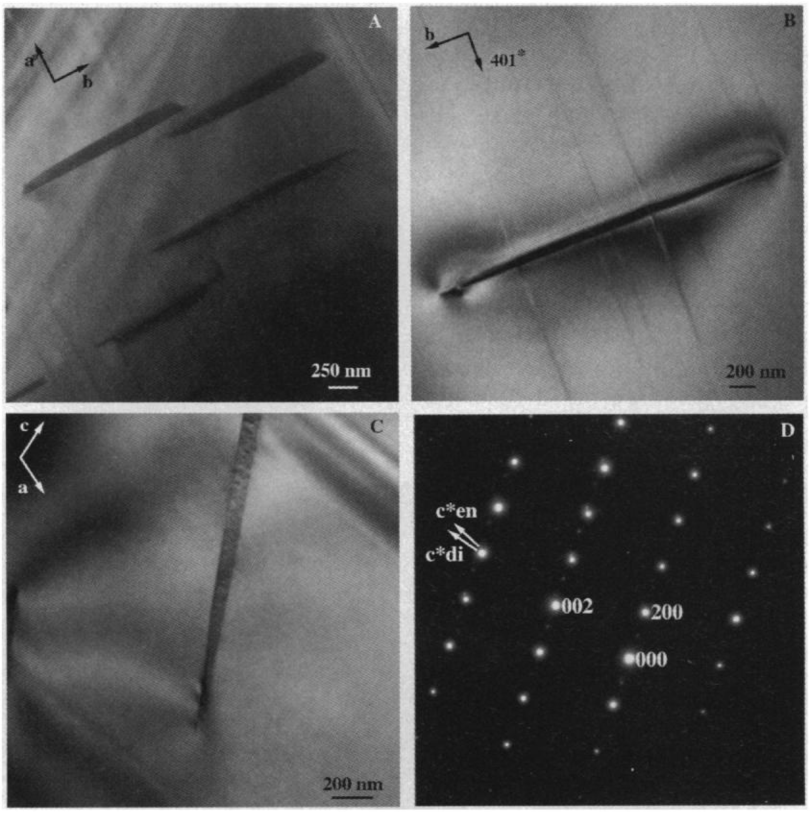

Fig. 1. Transmission electron micrographs of clinoenstatite exsolution lamellae in diopside from Alpe Arami lherzolite imaged down the *c* axis (**A**), parallel to the lamellae (**B** and **C**) and down the *b* axis (C). Very thin linear features parallel to (010) are retrograde amphibole slabs. Clinoenstatite lamellae are elongated at about 22° to (100) of diopside and show mottled contrast within them due to strain (C). Interfaces between host and lamellae are coherent except for rare dislocations located at or near the tips of some lamellae and associated with strain concentrations (B) and (C). The selected area electron diffraction (SAED) pattern (**D**) consists of [010] zone axis patterns of both the *C*-centered diopside (strong spots) and the $P2_1/c$ clinoenstatite (weak spots). Note that the spots with $h + k$ = even are present for both pyroxenes, whereas the spots with $h + k$ = odd are absent for the diopside host. Lattice misorientation between diopside (di) and clinoenstatite (en) is visible on the SAED pattern; the angles between the crystal axes of the two phases are about 2° for the c^* axes (labeled) and 1° for the a^* axes.

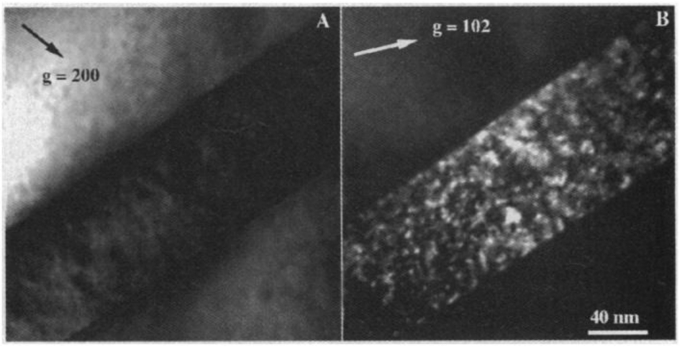

Fig. 2. A pair of dark-field images of a single clinoenstatite lamella in diopside matrix with operating reflections $h + k$ = even (**A**) and $h + k$ = odd (**B**). The mottled contrast within the lamella in (A) is like that seen in bright-field illumination (Fig. 1C) and is due to elastic lattice distortions (Fig. 3). Neither the shape nor size of the bright areas (domains of the primitive lattice) correlates with the strain-induced contrast features in (A). The diopside host appears bright in (A) because of the overlap of diopside and $h + k$ = even clinoenstatite reflections.

the criterion of antiphase domains, original exsolution of this phase is capable of explaining the lamellae we describe here, because the transformations from $C2/c$ structures to Lclen are displacive transformations that maintain the same point group symmetry ($2/m$) and approximate unit cell while reducing the translational symmetry from C to P (*21*). HTclen is stable only at low pressures and very high temperatures (*14*, *18*, *22*). It forms in basic volcanic rocks and then is transformed to Lclen during cooling, leaving the telltale antiphase domains (*15*). HTclen has also been produced in experiments (*22*), yielding the same transformed Lclen phase and antiphase domains upon quenching. In addition, extensive study of HTclen exsolution (*15*, *17*) has led to understanding of why the exsolution lamellae generally lie on high-index planes and how the orientation of the chosen planes varies with the lattice parameters of host and lamellae [which, in turn, are functions of composition and of the physical conditions of exsolution (*17*)]. On the basis of these data, one can calculate the orientation of the exsolution lamellae that would have been produced if the lamellae of Alpe Arami had exsolved as HTclen. Such lamellae could have a range of orientations depending on the specific conditions of exsolution, but in all cases the lamellae would be parallel to $h0\bar{l}$ of the host, a prediction verified by experiment (*22*). In contrast, the lamellae in diopside of Alpe Arami (Fig. 1C) are parallel to ($h0l$) and therefore cannot have precipitated originally as HTclen.

HPclen also crystallizes in SG $C2/c$ and therefore also is consistent with the existence and type of antiphase domains in the Lclen lamellae reported here. However, the lattice parameters of diopside and HPclen are not known as full functions of pressure, temperature, and composition, hence the same kind of quantitative calculations that can be performed for HTclen (*17*) cannot be performed. Verification of the orientation of HPclen lamellae in diopside must await further experimental data.

In addition to the four possible origins discussed above, one could postulate that these lamellae formed by metastable exsolution in the stability field of orthoenstatite, although there are no positive indications that such might be the case. There have been proposals of metastable exsolution of Fe-rich clinoenstatite previously (*23*) but not of Fe-poor clinoenstatite as is discussed here. Such formation is inconsistent with the evidence in this case, because of the following facts. (i) In no case of presumed metastable exsolution of clinoenstatite have antiphase domains been reported, hence there is no demonstration of metastable exsolution of any Ca-poor $C2/c$ pyroxene. (ii) In TEM studies of proposed metastable exsolution of clinoenstatite, clino- and orthoenstatite form intergrowths or possess high densities of stacking faults or twins parallel to (100) (or both), which are features not seen in Alpe Arami clinoenstatite lamellae. (iii) Exsolution of orthoenstatite from diopside in peridotites from both ophiolites and xenoliths is commonplace and has been reported for many years; the sole report of exsolution of clinoenstatite from diopside involves Alpe Arami (*9*). (iv) As mentioned above, there are two microstructural environments of diopside in Alpe Arami lherzolite (clumped within and around garnets, and distributed in the enstatite + olivine matrix), yet only the former exhibits clinoenstatite exsolution. Given that both sets of pyroxene have the same composition and that they participate in the cation exchange reactions that lead to assignment of a 5-GPa, 1300 to 1400 K former equilibrium (*24–26*), precipitation of HPclen in one population but not the other would have had to occur before the establishment of that equilibrium. Thus, the only conditions available for metastable exsolution are above 1300 K, which are temperatures where orthoenstatite easily exsolves from diopside in nature.

Based on these structural and crystal chemical arguments, only HTclen and HPclen are possible candidates for the originally exsolving phase, and only stable exsolution of HPclen is consistent with all of the data. In addition to these arguments, it is possible to use geological information to distinguish between HTclen and HPclen as the originally precipitating phase. In order for HTclen to have precipitated from diopside, the Alpe Arami lherzolite would have had to experience the conditions necessary to stabilize that phase (>1800 K, <1 GPa) (*12*, *13*, *16*, *20*) during exhumation. However, the documented conditions experienced by this peridotite on its way to the surface involved temperatures of 1200 to 1400 K at 130 to 160 km (4 to 5 GPa) (Fig. 4) (*24–26*) and at most 1100 K at 2 GPa (60 km depth) (*24–26*). These conditions are much too cold to have accessed the HTclen stability field (*14*, *15*, *18*). Confirmation of this conclusion comes from knowledge that the massif would have had to be melted to a large degree (its solidus under these conditions, even if anhydrous, would be less than 1600 K), which would probably have led

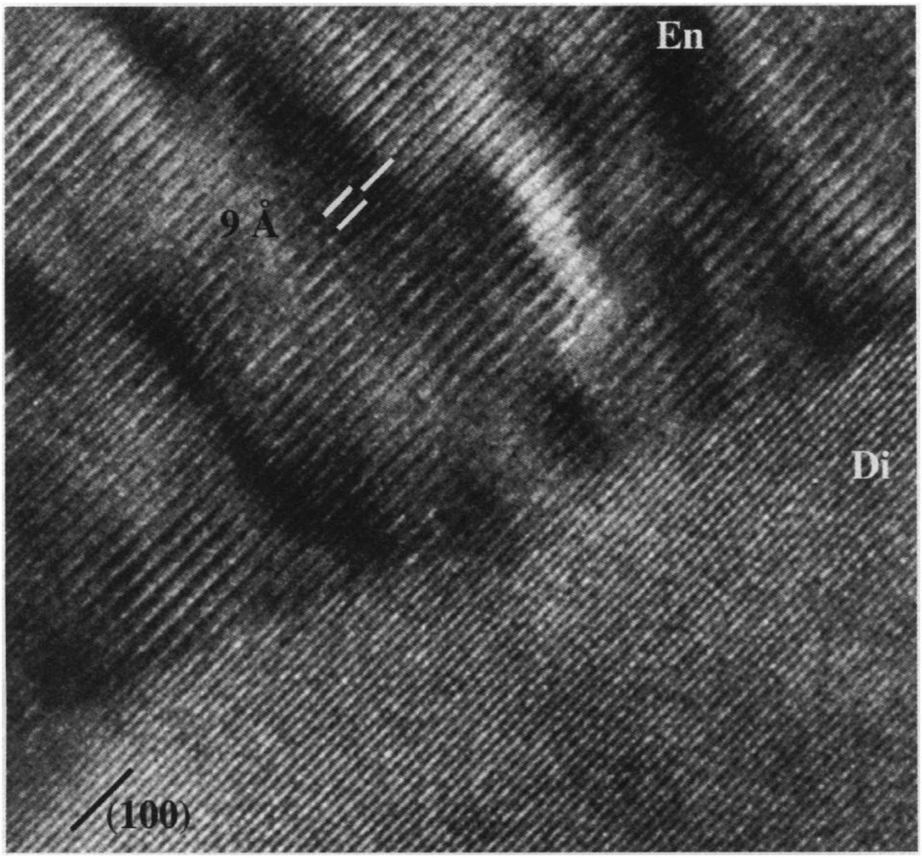

Fig. 3. HRTEM image including the interface between the diopside host (Di) and a clinoenstatite (En) lamella viewed down the b axis (as in Fig. 1C). The (100) lattice fringes of diopside are spaced ~4.7 Å apart as compared to ~9Å in clinoenstatite. The interface is coherent; ledges spaced about two to three unit cells apart are responsible for the general orientation of the phase boundary at ~20° from the c axis. The antiphase domain boundaries are revealed by abrupt $1/2a$ steps (marked by white lines) in the (100). The apparent width of the boundaries suggests that they are inclined with respect to the b axis. Elastic lattice distortions are visible as areas of mottled contrast similar to those seen in Figs. 1C and 2A and by rotation and bending of the lattice fringes. These distortions are also superimposed on the domain structure. The diopside part is free of defects and shows little elastic distortion on this scale.

to melt extraction; at minimum, it would have left a dominant igneous signature in the microstructure. Moreover, at shallow depths on such a high-temperature trajectory, the garnets would have been converted to pyroxene + spinel symplectites, and the high pressure thermobarometric signature of the massif as well as mineralogical and textural vestiges of the Alpine metamorphism preserved in the rocks (*5*, *7*, *9*) would have been seriously modified or erased.

In contrast, if the massif came from depths greater than the high-pressure Oren/HPclen phase boundary (*13*) along a trajectory consistent with the exhumation curve of Brenker and Brey (*26*), exsolution of an enstatite component from diopside at pressures in excess of the phase boundary would have been in the form of HPclen (Fig. 4) and would be consistent with all other observations concerning this peridotite. Of course, if equilibrium had been maintained during continued upward movement, the exsolution lamellae would have converted to Oren. We attribute the absence of this conversion to a combination of the following elements. (i) The coherent boundaries between the HPclen lamellae and the host combined with the reconstructive nature of the $C2/c \rightarrow$Oren transformation, which makes for a high activation energy of the reaction. (ii) The low-energy boundary between diopside and Oren is parallel to (100), far from (401), hence extensive rotation of lamellae would be required to retain a low-energy configuration. (iii) Slowing reaction kinetics at these moderate temperatures makes all reactions more sluggish. Thus, the work required to provide the activation free energy for the HPclen→Oren transformation would have been large. Instead, continuing exsolution of $(Mg,Fe)SiO_3$ occurred through the growth of rare orthoenstatite lamellae parallel to (100). At some undetermined lower temperatures and pressures, the unquenchable $C2/c \rightarrow P2_1/c$ reaction (*14*) ran within the HPclen lamellae, yielding the observed antiphase domains. The strong strain inhomogeneities that exist inside the lamellae are lacking in volcanic rocks (*15*, *17*). That probably is at least in part because of the abrupt volumetric expansion (~3%) between HPclen and the Lclen inversion product, whereas diopside parameters vary smoothly with pressure and temperature (*27*). The much larger scale bending in the diopside due to strain concentrated at the lamellae tips (Fig. 1, B and C), also is probably a consequence of the volumetric expansion upon transformation to Lclen.

The diopside crystals of Alpe Arami lherzolite that are not spatially associated with garnets have neither clinoenstatite lamellae nor the large elastic strains that are present in the garnet-associated diopsides, which suggests that they grew or recrystallized at lower pressures. This observation implies that the chemistry of these phases cannot be used to calculate conditions of origin of the lamellae, because cation exchange among all of the phases must have continued after formation of the lamellae. This is also the reason that thermobarometric analysis records pressure and temperature conditions experienced subsequent to the microstructures reported here. However, once a full set of lattice parameters as a function of pressure and temperature are available for HPclen and diopside, it should be possible to calculate the set of conditions and compositions that are consistent with exsolution of coherent lamellae that form approximately parallel to (401) of the host (*17*).

We conclude that exsolution of HPclen from diopside at very high pressure is consistent with all of the observations and that other interpretations would require additional assumptions, such as postulation that the strain domains in Fig. 2A are mimicking antiphase domains in Fig. 2B by some unknown process for which there is no direct evidence. The minimum depth of origin of these rocks is therefore probably determined by the location of the phase boundary between HPclen and Oren. The available data indicate that Ca displaces the boundary to slightly higher pressures relative to the Ca-free system (*28*), in part because the M sites of HPclen and Oren are similar in size (*14*). We make the conservative assumption that the effect of Ca is negligible and adopt the phase diagram for composition $(Mg_{0.9}Fe_{0.1})SiO_3$ (*29*), which fits our observations and represents a typical mantle composition (Fig. 4). Because it is clear that cations remained mobile during and after the conditions of exsolution of HPclen in Alpe Arami, it is not possible to estimate the conditions of exsolution within the HPclen field. However, the composition of diopside-enstatite solid solutions shown in figure 4 of Herzberg and Gasparik (*28*) suggests an upwelling path for Alpe Arami as shown in Fig. 4, which represents a slightly higher temperature gradient than that suggested in (*1*). Lower temperatures of origin would not be consistent with solubility trends of $MgSiO_3$ in diopside (*28*), because they would require heating during upwelling. Higher temperature paths imply higher pressures of origin.

The present study constrains only the trajectory of upwelling and the minimum depth of origin; we can place no constraints on the maximum depth experienced by these rocks. Also shown in Fig. 4 are the experimental conditions under which the solubility of TiO_2 in olivine in ilmenite-saturated lherzolite exceeds 0.6 weight % (*30*). Thus, the exhumation curve consistent with exsolution of HPclen from diopside indicates that olivine coexisting with diopside under conditions of HPclen exsolution could have had high dissolved TiO_2 if the bulk composition were appropriate. Whether or not the solubility data are applicable to Alpe Arami remains open because of the dispute about the TiO_2 content of olivine (*8*); if the image analysis data are correct, the intersection of the long arrow in Fig. 4 with the dashed line near 10 GPa and 1650 K is the deepest point that can be associated with this peridotite at this time. If the broad-beam microprobe data are correct, the peridotite must have been greatly undersaturated in ilmenite, and no maximum depth can be estimated. Still to be reconciled with these observations are the rod shape of titanates exsolved from olivine, the unique olivine LPO (*5*), and the spatial association of diopside and garnet (*1*, *31*).

Although the microstructures show that the very deep features are older than the Alpine orogeny, we have little constraint on the time of their formation. Zircons extracted from the massif have been dated at 465, 623, 650, and 1720 million years ago (Ma) (*32*). Thus, some of the microstructures could be much older than the Tertiary Alpine orogeny

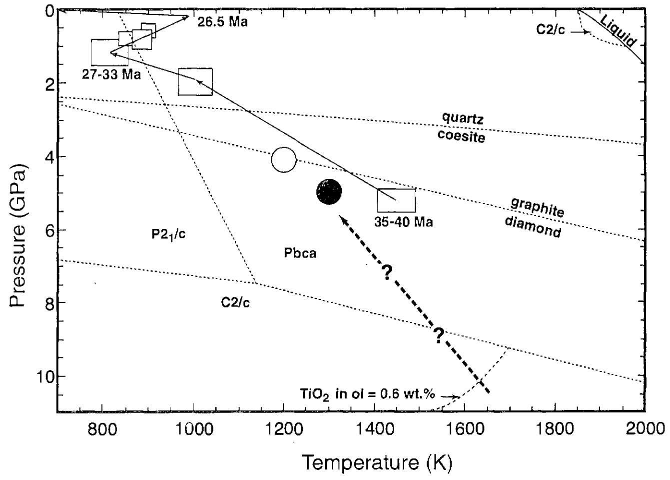

Fig. 4. Constraints on the exhumation path of the Alpe Arami peridotite. Open and solid circles represent maximum metamorphic conditions determined by Ernst (*24*) and by Medaris and Carswell (*25*), respectively, using thermobarometry. The exhumation curve from 5 GPa to the surface (boxes connected by solid arrows) is from Brenker and Brey (*26*) and references therein. The $(Mg_{0.9}Fe_{0.1})SiO_3$ phase diagram is from (*29*), and the HTclen stability field is from (*18*); the pyroxene phase fields are labeled with the SG of the stable phase. The solubility of TiO_2 in olivine is from (*30*). The dashed arrow below 5 GPa is a possible exhumation path consistent with data currently available.

(Variscan?), and the deeper parts of transport are conceivably not directly associated with a subduction zone. Recent discovery of pyroxene exsolution from garnets in peridotites of the Western Gneiss Region of Norway records depths of equilibration of at least 185 km (*33*), confirming that microstructural memory can extend to conditions deeper than those recorded by thermobarometry. The Norwegian rocks also yield radiometric dates suggesting that the peridotites are older than the Caledonian orogeny that brought them to the surface. In neither the Alpine nor Caledonian case is it clear what this disparity in time signifies, but it is clear that some process or series of processes exists that can transport rocks from depths of 200 km or more while preserving the memory of those conditions. We presume that the key to exhumation from such depths is continental collision accompanied by deep subduction of continental lithologies, but other than the pressure-temperature trajectory within the peridotites, the rocks themselves have so far yielded no direct information on this process.

References and Notes

1. L. Dobrzhinetskaya, H. W. Green II, S. Wang, *Science* **271**, 1841 (1996).
2. D. Mosely, *Am. Mineral.* **66**, 976 (1981); H. W. Green II and Y. Gueguen, *Tectonophysics* **92**, 71 (1983); M. R. Drury and H. L. M. van Roermund, *Geology* **16**, 1035 (1988); *ibid.* **17**, 676 (1989).
3. R. L. Hervig, J. V. Smith, J. B. Dawson, *Edinb. Trans. Earth Sci.* **77**, 181 (1986).
4. H. W. Green II, L. Dobrzhinetskaya, E. M. Riggs, Z.-M. Jin, *Tectonophysics* **279**, 1 (1997).
5. J. R. Möckel, *Leidse Geol. Med.* **42**, 61 (1969); J. M. A. Buiskool Toxopeus, *ibid.* **51**, 1 (1976); *Neues Jahrb. Miner. Abh.* **129**, 233 (1977a); *Tectonophysics* **39**, 55 (1977b); E. Den Tex, *Fortschr. Miner.* **48**, 69 (1971).
6. A. Nicolas and J.-P. Poirier, *Crystalline Plasticity and Solid State Flow in Metamorphic Rocks* (Wiley, New York, 1976); H .W. Green II and S. V. Radcliffe, *Earth Planet. Sci. Lett.* **15**, 239 (1972); *Geophys. Monogr.* **16**, 139 (1972); Y. Gueguen, *Tectonophysics* **39**, 231 (1977); Z.-M. Jin, H. W. Green II, R. S. Borch, *ibid.* **169** 23 (1989).
7. C. B. Raleigh, *J. Geophys. Res.* **73**, 5391 (1968); N. L. Carter and H. G. Ave'Lallement, *Geol. Soc. Am. Bull.* **81**, 2181 (1970); D. L. Kohlstedt and C. Goetze, *J. Geophys. Res.* **79**, 2045 (1974); W. Durham, C. Goetze, B. Blake, *ibid.* **82**, 5755 (1977); D. H. Zeuch and H. W. Green II, *Tectonophysics* **110**, 263 (1984); H. W. Green II, in *Electron Microscopy in Mineralogy*, H.-R. Wenk *et al.*, Eds. (Springer-Verlag Berlin, Heidelberg, 1976), pp. 443–464.
8. A. C. Risold, V. Trommsdorff, E. Reusser, P. Ulmer, B. Grobety, *Trans. AGU* **77**, F761 (1996); A. C. Risold, V. Trommsdorff, E. Reusser, P. Ulmer, M. Pfiffner, *Eur. Geophys. Union* **9**, 93 (1997); B. Hacker, T. Sharp, R. Y. Zhang, J. G. Liou, R. L. Hervig, *Science* **278**, 702 (1997); H. W. Green II, L. Dobrzhinetskaya, K. Bozhilov, *ibid.*, p. 704.
9. Y. Yamaguchi, J. Akai, K. Tomita, *Contrib. Mineral. Petrol.* **66**, 263 (1978).
10. Doubly polished 30-μm-thick sections were prepared, portions of which were mounted on single-hole diamond grids and ion milled at 5 kV with argon plasma beams until the sample was perforated. TEM was performed at the University of California, Riverside, on a Philips CM300 transmission electron microscope operating at an accelerating voltage of 300 kV and equipped with an EDAX energy dispersive spectrometer with Si detector and super-ultrathin window, which allows detection and quantification of light elements such as oxygen. The parameterless method of E. Van Cappellen [*Microsc. Microanal. Microstruct.* **1**, 1 (1990)] was used to determine experimental *k* factors, and the quantification procedure included a thickness correction assuming stoichiometry of oxygen [E. Van Cappellen and J.-C. Doukhan, *Ultramicroscopy* **53**, 343 (1994)].
11. K. N. Bozhilov, H. W. Green II, L. Dobrzhinetskaya, data not shown.
12. The amphibole structure was confirmed by electron diffraction and HRTEM imaging. The amphibole slabs are typically one to two unit cells thick parallel to *b*; in rare cases they reach a thickness of about 10 unit cells. In some cases, generally near the clinoenstatite lamellae tips, the amphibole slabs traverse the lamellae. Mostly, however, they run up to the lamellae boundaries and go around them, as typically observed during the hydration of complex exsolved pyroxenes [D. R. Veblen and P. R. Buseck, *Am. Mineral.* **65**, 599 (1980), D. R. Veblen and D. L. Bish, *ibid.* **73**, 677 (1988), K. J. T. Livi and D. R. Veblen, *ibid.* **74**, 1070 (1989)].
13. Viewed down *b*, brightfield images and darkfield images with $h + k$ = even show very similar mottling of contrast within clinoenstatite lamellae; the size, shape, and orientation of contrast domains are the same. Figure 3 shows that this mottling is primarily due to inhomogeneous elastic distortion. For example, the (100) fringes in the brightest region of Fig. 3 are rotated clockwise relative to the domains on either side of it. There are no crystal defects associated with the boundaries of the bright region. In addition, the fringe terminations do not show long-range strain fields; they do not represent dislocations. Therefore, the fringe offsets are growth features; symmetry rules forbid them to be a consequence of elastic strain.
14. M. Cameron and J. J. Papike, *Am. Mineral.* **66**, 1 (1981); R. E. G. Pacalo and T. Gasparik, *J. Geophys. Res.* **95**, 15853 (1990); R. J. Angel, A. Chopelas, N. L. Ross, *Nature* **358**, 322 (1992); R. J. Angel and D. A. Hugh-Jones, *J. Geophys. Res.* **99**, 19777 (1994); D. Hugh-Jones, A. B. Woodland, R. J. Angel, *Am. Mineral.* **79**, 1032 (1994); D. Hugh-Jones, T. Sharp, R. Angel, A. Woodland, *Eur. J. Mineral.* **8**, 1337 (1996).
15. N. Morimoto and M. Tokonami, *Am. Mineral.* **54**, 725 (1969); J. C. Bailey *et al.*, *Proc. Apollo 11 Lunar Sci. Conf.* **1**, 169 (1970); G. L. Nord, A. H. Heuer, J. S. Lally, in *Electron Microscopy in Mineralogy*, H.-R. Wenk, Ed. (Springer-Verlag, New York, 1976), pp. 220–227; M. A. Carpenter, *Phys. Chem. Miner.* **5**, 119 (1979); P. R. Buseck, G. L. Nord, D. R. Veblen, in *Pyroxenes, Reviews in Mineralogy*, C. T. Prewitt Ed. (Mineralogical Society of America, Washington, DC, 1980), pp. 117–211; K. T. J. Livi and D. R. Veblen, *Am. Mineral.* **74**, 1070 (1989).
16. The exsolution of pigeonite lamellae in augite (diopside is augite with a composition close to $CaMgSi_2O_6$, and pigeonite is clinoenstatite with a small Ca component) and vice versa is a well-known phenomenon (*14, 15, 17, 19*). Augite and pigeonite are respectively Ca-rich and Ca-poor pyroxenes that show limited solid solution between them; both also have a significant Fe content. There is a considerable literature on the $C2/c \rightarrow P2_1/c$ transformation in basic volcanic rocks in which subcalcic augite (space group *C2/c*) first crystallizes from the magma and then inverts to pigeonite (space group $P2_1/c$). A similar transformation takes place in multianvil experiments upon decompression of HPclen (*14*), which also has the *C2/c* space group but has a different structure and topology from augite. It has not been possible to retain this phase in low-Fe pyroxenes during decompression; room-temperature decompression induces the $C2/c \rightarrow P2_1/c$ transformation with an overstepping of the phase boundary by ~1 GPa (*14*). The most striking differences between HTclen and HPclen are in density ($\Delta\rho \sim 3\%$) and in the different degree of kinking of the silicate tetrahedral chains [expressed macroscopically as different angles of monoclinicity (β) ~110° in HTclen and ~101° in Hpclen].
17. P. Robinson, M. Ross, G. L. Nord Jr., J. R. Smyth, H. W. Jaffe, *Am. Mineral.* **62**, 857 (1977).
18. T. Gasparik, *ibid.* **75**, 1080 (1990).
19. S. Iijima and P. R. Buseck, *ibid.* 60, 758 (1975); P. E. Champness and P. A. Copley, in *Electron Microscopy in Mineralogy*, H.-R. Wenk, Ed. (Springer-Verlag, New York, 1976), pp. 228–233.; H. Boysen, F. Frey, H. Schrader, G. Eckold, *Eur. J. Mineral.* **17**, 629, (1991).
20. R. S. Coe and S. H. Kirby. *Contrib. Mineral. Petrol.* **52**, 29 (1975).
21. G. L. Nord Jr., *Rev. Mineral.* **27**, 455 (1992).
22. H. Feuer, L. Schöpfer, H. Fuess, D. A. Jefferson, *Eur. J. Mineral.* **1**, 507 (1989).
23. H. W. Jaffe, P. Robinson, R. J. Tracy, *Am. Mineral.* **60**, 9 (1975); F. J. Rietmeijer and P. E. Champness, *Min. Mag.* **45**, 11, (1982).
24. W. G. Ernst, *J. Petrol.* **19**, 341 (1978); W. G. Ernst, *Am. Mineral.* **66**, 443 (1981).
25. L. G. Medaris and D. A. Carswell, in *Eclogite Facies Rocks*, D. A. Carswell, Ed. (Blackie, Glasgow, UK, 1990), pp. 260–290; H. Becker, *Geology* **21**, 599 (1993).
26. F. E. Brenker and G. P. Brey, *J. Metamorph. Geol.* **15**, 581 (1997).
27. The generally close association between the boundaries of strain domains and arrays of lattice fringe offsets within clinoenstatite lamellae suggests a relationship between them. Figure 1, B and C, and Fig. 2A show that the scale of strain inhomogeneity in the lamellae is grossly different from that in the host and that the latter is related to the presence of the lamellae. There are no similar strain effects in diopside crystals that lack clinoenstatite lamellae, nor are such effects present within or around amphibole lamellae. A natural explanation for these correlations and the strain itself is the possibility that the strain pattern is a consequence of the 3% volume expansion that accompanies the HPclen→Lclen inversion. Multiple nucleation sites of the stable phase along the host-daughter interface would lead to "puckering" of the lattice due to local anisotropic expansion in a lamella contained within an essentially rigid framework (its coherent boundaries with the host). The regions of greatest curvature could, in turn, prejudice nucleation of additional antiphase domains. This scenario, although not a proven process, is consistent with the available evidence and provides a reasonable explanation for the pattern of strain and its relationship to the antiphase boundaries.
28. C. Herzberg and T. Gasparik, *J. Geophys. Res.* **96**, 16263 (1991); A. B. Woodland and H. St. C. O'Neill, *Contrib. Mineral. Petrol.* **121**, 87 (1995).
29. A. B. Woodland and R. J. Angel, *Eur. J. Mineral.* **9**, 245 (1997); A. B. Woodland, *Geophys. Res. Lett.* **25**, 1241 (1998).
30. L. Dobrzhinetskaya, K. N. Bozhilov, H. W. Green II, *Chem. Geol.*, in press. Reversed experiments were conducted on nominally anhydrous ilmenite-saturated lherzolite compositions at pressures from 5 to 12 GPa and temperatures from 1400 to 1700 K. Crystals were analyzed by electron beam microanalysis by scanning electron microscopy and TEM, and the lack of submicroscopic inclusions was demonstrated. Concentrations of TiO_2 in olivine were recorded ranging from <0.1 weight % at 1400 K and 5 GPa to >1.0 weight % at 1700 K and 12 GPa. TiO_2 concentrations of 0.6 weight % or more in olivine were measured for temperature >1650 K at 10 GPa and temperature ≥1500 K at 12 GPa.
31. S. E. Haggerty, *Eos Trans. AGU* **75**, 192 (1994).
32. D. Gebauer, M. Grunenfelder, G. R. Tilton, V. Trommsdorff, *Terra Abstr.* **6**, 5 (1993); D. Gebauer, *1st Workshop on UHP Metamorphism and Tectonics*, abstract A-67 (Stanford University, Stanford, CA, 1994).
33. H. L. M. van Roermund and M. R. Drury, *Eos Trans. AGU* **79**, F971 (1998); H. L. M. van Roermund, M. R. Drury, A. Barnhoorn, A. De Ronde, *Terra Nova*, in press.
34. This work was partially supported by NSF grants EAR94-13517 and EAR96-283432. We thank R. J. Angel, F. E. Brenker, W. G. Ernst, B. Hacker, G. Nord, C. Prewitt, P. Robinson, N. L. Ross, T. Sharp, H. L. M. van Roermund, A. B. Woodland, and two anonymous reviewers for helpful discussions and suggestions.

22 December 1998; accepted 23 February 1999